pair between equivalent
des between K points are
py on the tube due to its
ing energy that depends
on localization length ξ_n
measures the anisotropy
localization length leads
in(3θ). We calculate the
contributions from the

$$+B\frac{n^2}{R^2}\Bigg)\sin(3\theta)$$
$$\frac{(R)n}{ER}\sin(3\theta) \qquad (2)$$

he Coulomb anisotropy,
Table 2 we compare the
e experimental data with
dicts a nonlinear scaling
here the nonlinearity has
d suppressing the positive
(2) shows that as the
fies the effects of trigonal
nparable contributions to

under Grant DE-FG-02-
grant DMR-00-79909. We
ns.

Review Letters)

Tubular Image States and Light-Driven Molecular Switches

Petr Král[1,2], Brian Granger[2], H. R. Sadeghpour[2], Ioannis Thanopulos[1], Moshe Shapiro[1] and Doron Cohen[3]

[1] *Department of Chemical Physics, Weizmann Institute of Science, Israel*
[2] *ITAMP, Harvard-Smithsonian Center for Astrophysics, Cambridge, Massachusetts 02138*
[3] *Department of Physics, Ben-Gurion University, Beer-Sheva, Israel*

Abstract. We introduce new tubular image states (TIS) that can be formed around linear conductors and dielectrics, like metallic carbon nanotubes. These Rydberg-like molecular states have a very large extent and possess peculiar physical properties. We also present a two-step light-driven enantiomeric switch, which within 100 ns can turn a mixture of left and right chiral molecules into a pure enantiomeric form. Molecular switches with more quasi-stable states can be used as dynamic memories or motors.

Today's nanotechnology operates at the crossroad between physics, chemistry and biology. The prepared molecular-scale systems fulfill various complex tasks, like chemical nano-sensing or providing of motoric activity. Coherent transport regimes can often be present in these systems, since their scale is too small for a proper relaxation to occur. We discuss two examples of such unique systems.

TUBULAR IMAGE STATES

Large Rydberg states with long lifetimes can be observed in atoms and molecules. Extended electronic image states can be also observed above bulk conductors or dielectrics, clusters and liquid He. Their Coulomb-like potential $V(\rho) = -\frac{e^2}{4\rho}\left(\frac{\epsilon-1}{\epsilon+1}\right)$ gives binding energies $E_n = -\frac{13.60}{16n^2}\left(\frac{\epsilon-1}{\epsilon+1}\right)^2$ eV=15-40 meV. Practical application of these states is usually limited by their picosecond lifetimes, mostly given by their spatial overlap with the surface states.

Recently, we have suggested a new class of "tubular image states" (TIS), formed above freely suspended linear molecular conductors or dielectrics [1]. These TIS have a *non-zero angular momentum l*. The resulting centrifugal forces keeps the wave functions away from the surface, so the TIS population becomes stabilized against collapse on the nanotube, rendering it long living at low temperatures.

CP685, *Molecular Nanostructures: XVII Int'l. Winterschool/Euroconference on Electronic Properties of Novel Materials*, edited by H. Kuzmany, J. Fink, M. Mehring, and S. Roth

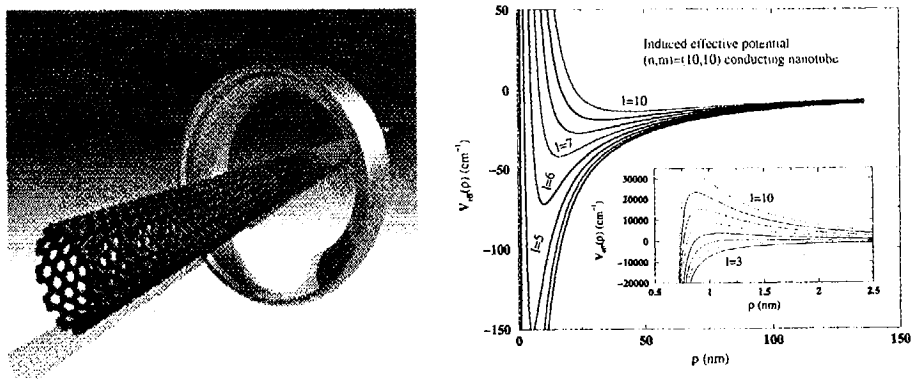

FIGURE 1.

In Fig. 1 (left), we show a visualization of an idealized TIS around a $(10, 10)$ metallic carbon nanotube of radius $a = 0.68$ nm. External electron is *attracted* to the material surface by its image charge and *repulsed* by its angular momentum, so the states are formed in quantum wells separated from the surface (right).

In the first approximation, we can model the linear conductor by a metallic cylinder of radius a. Point charge, at distances $\rho_0 \gg a$ above the cylinder, has a potential Φ_0, that polarizes the tube and induces the potential Φ_{ind}. The total potential $\Phi_{tot} = \Phi_0 + \Phi_{ind}$ vanishes at the nanotube surface, that results in

$$\Phi_{ind}(\rho, \varphi, z) = -\frac{2q}{\pi} \sum_{m=-\infty}^{m=+\infty} \int_0^\infty dk \, \cos(kz) \, \exp(im\phi) \times \frac{I_m(ka)}{K_m(ka)} K_m(k\rho_0) \, K_m(k\rho) \, . \tag{1}$$

The electron potential energy is given by $V(\rho_0) = \frac{1}{2} q \, \Phi_{ind}(\rho_0, 0, 0)$. At $\rho_0 \gg a$ we can find the attractive potential ($\mathrm{li(x)} \equiv \int_0^x \mathrm{dt}/\ln(\mathrm{t})$)

$$V(\rho_0) \sim \frac{q^2}{a} \, \mathrm{li}\left(\frac{\mathrm{a}}{\rho_0}\right) \approx -\frac{\mathrm{q}^2}{\mathrm{a}} \frac{1}{(\rho_0/\mathrm{a}) \ln(\rho_0/\mathrm{a})} \, , \tag{2}$$

which interpolates the potential for a charge above a metallic plane, $V \sim -1/\rho$, and a sphere, $V \sim -1/r^2$. The effective potential of the electron has the attractive induced part and the repulsive centrifugal part, $V_{eff}(\rho) = V(\rho) + \frac{(l^2 - \frac{1}{4})}{2m_e \rho^2}$. For $l > 5$, the system develops extended but shallow quantum wells that support bound TIS, as shown in Fig. 1 (right). The collapse of their population on the tube is suppressed by the centrifugal barrier (see the inset).

The total TIS wave functions $\Psi_{n,l,k}(\rho, \varphi, z) = \psi_{n,l}(\rho) \, e^{il\varphi} \phi_k(z) / \sqrt{2\pi\rho}$ have the eigenenergies $E_{n,l,k} = E_{n,l} + E_k$, where $E_{n,l}$ is related with the radial electron motion and E_k is the kinetic energy for the axial motion along the tube. The radial wave functions $\psi_{n,l}(\rho)$ satisfy the Schrödinger equation

$$\left(\frac{d^2}{d\rho^2} + 2m_e \left[E_{n,l} - V_{eff}(\rho) \right] \right) \psi_{nl}(\rho) = 0 \, . \tag{3}$$

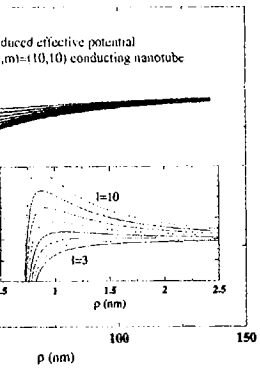

TIS around a (10, 10)
electron is *attracted* to
angular momentum, so
surface (right).
onductor by a metallic
above the cylinder, has
tential Φ_{ind}. The total
, that results in

$$p\,(im\phi)$$

(1)

$(\rho_0, 0, 0)$. At $\rho_0 \gg a$ we

(2)

allic plane, $V \sim -1/\rho$,
ctron has the attractive
$V(\rho) + \frac{(l^2-\frac{1}{4})}{2m_e\rho^2}$. For $l > 5$,
hat support bound TIS,
n the tube is suppressed

$^{il\varphi}\phi_k(z)/\sqrt{2\pi\rho}$ have the
e radial electron motion
e tube. The radial wave

(3)

In Fig. 2 (left), we show some of the states with $n = 1$. Their maxima are located at the distance $r_{max} \sim l^3$ (10 – 50 nm for $l > 5$) from the tube surface.

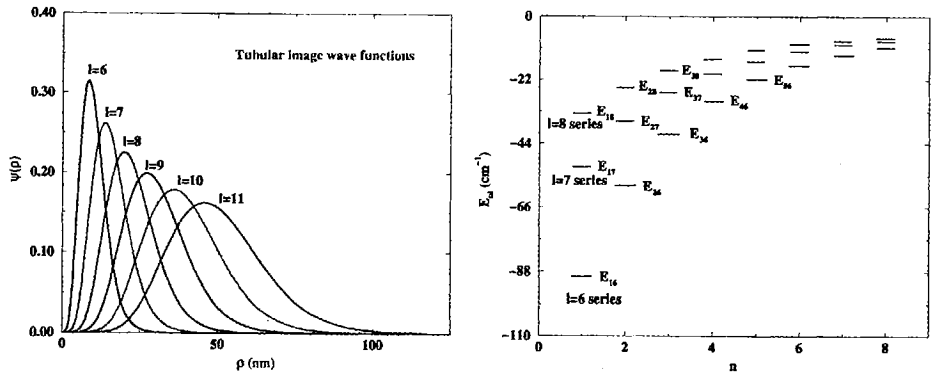

FIGURE 2.

In Fig. 2 (right), we show the eigenenergies $E_{n,l} \sim 1 - 10$ meV related with the radial motion. TIS with the same quantum number n but different angular momentum l are non-degenerate and scale as $E_{n,l} \sim l^{-3}$. They can be filled by radiative recombination, similarly as image states above bulk metals.

Presently, we also study TIS above several tubes and TIS with more electrons. Two TIS electrons spin in the same direction, on opposite sides of the tube circumpherence, and are shifted one from another along the tube to a distance, determined by an additional external potential.

LIGHT-DRIVEN MOLECULAR SWITCHES

Let us now discuss an optical "enantio-selective switch" [2], that, in two steps, turns a ("racemic") mixture of left-handed and right-handed chiral molecules into the enantiomerically pure state of interest. The switch is applied on the (transiently chiral) D_2S_2 molecule, shown schematically in Fig. 3 (left), together with a one-dimensional cut of the ground electronic potential energy surface along the enantiomutative path, with a few chiral and non-chiral ro-vibronic states.

The enantio-switch is composed of an "enantio-discriminator" and an "enantio-converter" acting in tandem. The enantio-discriminator is based on our "Cyclic Population Transfer" scheme (CPT) [3]. The approach is akin to the Adiabatic Passage (AP), used to *completely* transfer population between quantum states, that are optically coupled as, $|1\rangle \leftrightarrow |2\rangle \leftrightarrow |3\rangle$. In chiral molecules, lacking an inversion center and thus having eigenstates with ill defined parity, $|k\rangle_{L,D} = \frac{1}{\sqrt{2}}\left(|k\rangle_S \pm |k\rangle_A\right)$ $(k = 1, 2, 3)$, it is possible to close the "cycle" by introducing a third field which

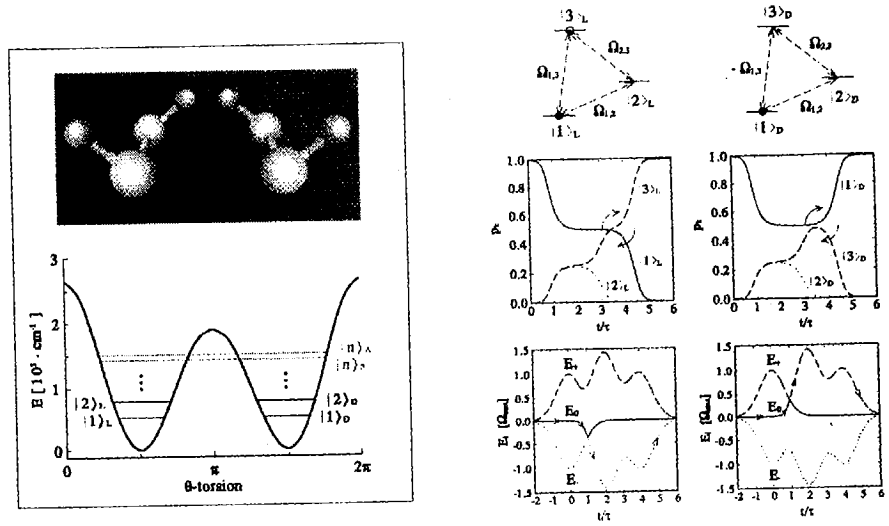

FIGURE 3.

couples the states $|1\rangle \leftrightarrow |3\rangle$ directly (see Fig. 3 (right top)). The interference of one and two-photon transitions along the two paths renders the evolution dependent on the total *phase* φ of the three coupling terms [3]. Since the transition dipoles of the two enantiomers differ in sign, their evolution under the action of the three fields is different, and the two can be *separated* and *converted* one to another.

We denote the levels in each enantiomer by $|i\rangle$, with their energies ω_i ($\hbar = 1$ in atomic units). The external electric field is chosen to be a sum of components, each being in *resonance* with one of the $|i\rangle \leftrightarrow |j\rangle$ transition frequencies of interest, $\mathbf{E}(t) = \sum_{i\neq j} \mathcal{R}_e\left[\hat{\epsilon}\,\mathcal{E}_{i,j}(t)e^{-i\omega_{i,j}t}\right]$, where $\omega_{i,j} = \omega_i - \omega_j$, and $\hat{\epsilon}$ is the polarization direction. The Hamiltonian of the system in the rotating wave approximation is,

$$\mathsf{H} = \sum_{i=1}^{3} \omega_i |i\rangle\langle i| + \sum_{i>j=1}^{3} \left(\Omega_{i,j}(t)e^{-i\omega_{i,j}t}|i\rangle\langle j| + \text{H.c.}\right). \tag{4}$$

It depends on the Rabi frequencies, $\Omega_{i,j}(t) = \mu_{i,j}\,\mathcal{E}_{i,j}(t)$, where $\mu_{i,j}$ are the transition-dipole matrix elements. Expanding the system wave function in the material states $|i\rangle$ as, $|\psi(t)\rangle = \sum_{i=1}^{N} c_i(t)\,e^{-i\omega_i t}\,|i\rangle$, the (column) vector of the slow varying coefficients $\mathbf{c} = (c_1, c_2, c_3)^{\mathsf{T}}$, with T designating the matrix transpose, is the solution of the matrix-Schrödinger equation $\dot{\mathbf{c}}(t) = -i\,\mathsf{H}(t)\cdot\mathbf{c}(t)$, where $\mathsf{H}(t)$ is the effective Hamiltonian matrix

$$\mathsf{H}(t) = \begin{bmatrix} 0 & \Omega^*_{1,2}(t) & \Omega^*_{1,3}(t) \\ \Omega_{1,2}(t) & 0 & \Omega^*_{2,3}(t) \\ \Omega_{1,3}(t) & \Omega_{2,3}(t) & 0 \end{bmatrix}. \tag{5}$$

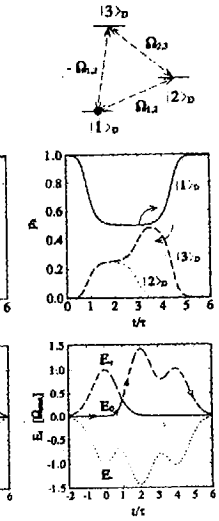

The interference of one
ıe evolution dependent
e the transition dipoles
the action of the three
ed one to another.
ıeir energies ω_i ($\hbar = 1$
a sum of components,
frequencies of interest,
d $\hat{\epsilon}$ is the polarization
vave approximation is,

$$\text{l.c.})\,. \tag{4}$$

$t)$, where $\mu_{i,j}$ are the
ı wave function in the
ımn) vector of the slow
he matrix transpose, is
$\mathsf{H}(t) \cdot \mathbf{c}(t)$, where $\mathsf{H}(t)$ is

$$(5)$$

The phases of the Rabi frequencies $\Omega_{i,j}(t)$ are given by $\phi_{i,j} = \phi^{\mu}_{i,j} + \phi^{E}_{i,j}$, where $\phi^{\mu}_{i,j}$ are the phases of the dipole matrix elements $\mu_{i,j}$, and $\phi^{E}_{i,j}$ are the phases of the electric field components $\mathcal{E}_{i,j}$. The evolution of the system is determined by the *total* phase $\varphi \equiv \phi_{1,2} + \phi_{2,3} + \phi_{3,1}$, which is shifted by π in the two enantiomers, since one or three of their Rabi frequencies $\Omega_{i,j}(t)$ are opposite (see Fig. 3).

The process applies a "dump" pulse $\mathcal{E}_{2,3}(t)$ that couples the $|2\rangle \leftrightarrow |3\rangle$ states and two subsequent "pump" pulses, overlapping with the dump pulse, that couple the $|1\rangle \leftrightarrow |2\rangle$ and the $|1\rangle \leftrightarrow |3\rangle$ states. The Rabi frequencies are $\Omega_{2,3}(t) = \Omega^{\max} f(t)$, $\Omega_{1,2}(t) = \Omega^{\max} f(t-2\tau)$, $\Omega_{1,3}(t) = \Omega_{1,2}(t) + \Omega^{\max} f(t-4\tau) \exp\{-i\,t\,\Omega^{\max} f(t-6\tau)\}$, where $\Omega^{\max} = 1\ \mathrm{ns}^{-1}$ and $f(t) = \exp[-t^2/\tau^2]$.

The population in both enantiomers initially follows the eigenstate $|E_0\rangle$ of the zero eigenvalue E_0 of the Hamiltonian (5). As the three Rabi frequencies get closer in magnitude, $|\Omega_{1,2}| = |\Omega_{1,3}| \approx |\Omega_{2,3}| = \Omega$, the eigenvalues E_0 crosses the eigenvalues E_- or E_+, depending on the enantiomer (see Fig. 3 (right bottom)). As a result, their population is *diabatically* transferred to the respective eigenstate $|E_+\rangle$ or $|E_-\rangle$, depending on the enantiomer. Next we adiabatically turn off the pulse $\mathcal{E}_{1,2}(t)$. Therefore, the zero adiabatic eigenstate $|E_0\rangle$ correlates adiabatically with state $|2\rangle$, which thus becomes *empty* after this process, while the occupied $|E_+\rangle$ and $|E_-\rangle$ states correlate to, $|E_\pm\rangle \to (|1\rangle \pm |3\rangle)/\sqrt{2}$.

The *chirp* in the second term of $\Omega_{1,3}(t)$ causes a $\pi/2$ *rotation* in the $\{|1\rangle, |3\rangle\}$ subspace at $t \approx 5\tau$. As a result, state $|E_+\rangle$ goes over to state $|3\rangle$ and state $|E_-\rangle$ goes over to state $|1\rangle$, or vice versa, depending on φ. The net result of the adiabatic passage and the rotation is that one enantiomer returns to its initial $|1\rangle$ state and the other switches over to the $|3\rangle$ state. As shown in the middle panel of Fig. 3, the enantio-discriminator is very *robust*, with all the population transfer processes occurring in a smooth fashion.

We then apply the "enantio-converter" process [2], based on other phase sensitive population transfer methods [4,5]. The process converts the excited $|3\rangle_L$ state to the $|4\rangle_D$ state, while going through two higher excited states as follows $|3\rangle_L \to \alpha\, e^{-i\omega_{5S}t}\,|5\rangle_S + \beta\, e^{-i\omega_{5A}t}\,|5\rangle_A \to |4\rangle_D$. Thus in the end all the molecules have the same symmetry. This methodology could lead to applications in organic chemistry, biochemistry and drug industry. Moreover, we are studying its application to Jahn-Teller molecules with more than two quasi-stable states. Such systems could applied in light-driven molecular motors and multi-state memories.

REFERENCES

1. B. Granger, P. Král, H. R. Sadeghpour and M. Shapiro, Phys. Rev. Lett. **89**, 135506 (2002).
2. P. Král, I. Thanopulos, M. Shapiro and D. Cohen, Phys. Rev. Lett. **90**, 033001 (2003).
3. P. Král and M. Shapiro, Phys. Rev. Lett. **87**, 3002 (2001).
4. P. Král and M. Shapiro, Phys. Rev. A **65**, 043413 (2002).
5. P. Král, Z. Amitay and M. Shapiro, Phys. Rev. Lett. **89**, 063002 (2002).